JOURNAL OF GEOPHYSICAL RESEARCH, VOL. 115, A04209, doi:10.1029/2009JA014677, 2010

Click Here for Full Article

Concerning the motion of flux transfer events generated by component reconnection across the dayside magnetopause

D. G. Sibeck[1] and R.-Q. Lin[2]

Received 24 July 2009; revised 25 October 2009; accepted 4 December 2009; published 15 April 2010.

[1] We generate flux transfer events (FTEs) along subsolar component reconnection curves whose tilt depends upon the interplanetary magnetic field (IMF) orientation, track their motion in response to pressure gradient and magnetic curvature forces, and estimate the perturbations they produce in the ambient magnetosheath and magnetosphere. During periods of southward IMF orientation, FTEs move poleward rapidly without ever reaching the flanks of the magnetosphere, while during periods of northward and duskward IMF they slip slowly over the flanks. Speeds increase when a depletion layer is present. For southward IMF orientations, the greatest magnetic field perturbations occur near the equator and diminish with distance from the posited reconnection line. For northward and duskward IMF orientations, dayside perturbation amplitudes are lower but increase with downstream distance at off-equatorial locations. Consequently events occurring for southward IMF orientations should dominate statistical surveys of dayside events but not those of flank events. The events move through the ambient media, invariably generating outward/inward flow perturbations in the magnetosheath but inward/outward perturbations in the magnetosphere. Multipoint spacecraft timing studies can be used to determine event axes and the component of event motion perpendicular to these axes. Because FTEs retain their initial orientations, timing studies afford an opportunity to determine the orientation of the dayside reconnection curve from remote locations.

Citation: Sibeck, D. G., and R.-Q. Lin (2010), Concerning the motion of flux transfer events generated by component reconnection across the dayside magnetopause, *J. Geophys. Res.*, *115*, A04209, doi:10.1029/2009JA014677.

1. Introduction

[2] Flux transfer events (FTEs) are common in the vicinity of the dayside and flank magnetopause, where they can be identified on the basis of brief (~1–2 min) isolated bipolar magnetic field signatures normal to the nominal magnetopause centered on enhanced magnetic field strengths [*Russell and Elphic*, 1978]. Because events on the dayside tend to occur for southward interplanetary and magnetosheath magnetic field orientations [*Rijnbeek et al.*, 1984; *Berchem and Russell*, 1984], they are generally interpreted in terms of bursty magnetic reconnection associated with current-driven instabilities at the magnetopause. However, similar events seen on the flanks exhibit no tendency to occur preferentially for southward interplanetary magnetic field (IMF) orientations [*Kawano and Russell*, 1997a].

[3] Several proposals seek to reconcile the differing occurrence patterns of events on the dayside and flank magnetopause with reconnection model predictions. One school of thought predicts that all events originate via component reconnection along lines passing through the vicinity of the subsolar magnetopause, but for one reason or another those occurring near local noon during periods of northward IMF orientation are difficult to observe. According to *Kawano and Russell* [1997b], this is because "rereconnection," or simultaneous reconnection at multiple sites, precludes event development and motion. Adopting a similar line of reasoning, *Sibeck* [2009] argued that events generated along a component reconnection line are difficult to observe because the amplitudes of the perturbations that they generate in the ambient magnetosheath and magnetospheric magnetic fields during periods of northward IMF orientation are far less than the amplitudes of the perturbations they generate during periods of southward IMF orientation. The other school of thought invokes two modes of reconnection to explain the differing dayside and flank event occurrence patterns. *Fear et al.* [2005] proposed that FTEs on the flanks originate via component reconnection on the dayside magnetopause during periods of southward IMF orientation but via antiparallel reconnection at high latitudes during periods of northward IMF orientation. Only events originating locally can be observed on the dayside, whereas events originating on both the dayside and at high latitudes reach the flanks.

[4] Models describing the motion and perturbations generated by FTEs as a function of IMF orientation are needed to

[1]NASA Goddard Space Flight Center, Greenbelt, Maryland, USA.
[2]Carderock Division, Naval Surface Warfare Center, West Bethesda, Maryland, USA.

This paper is not subject to U.S. copyright.
Published in 2010 by the American Geophysical Union.

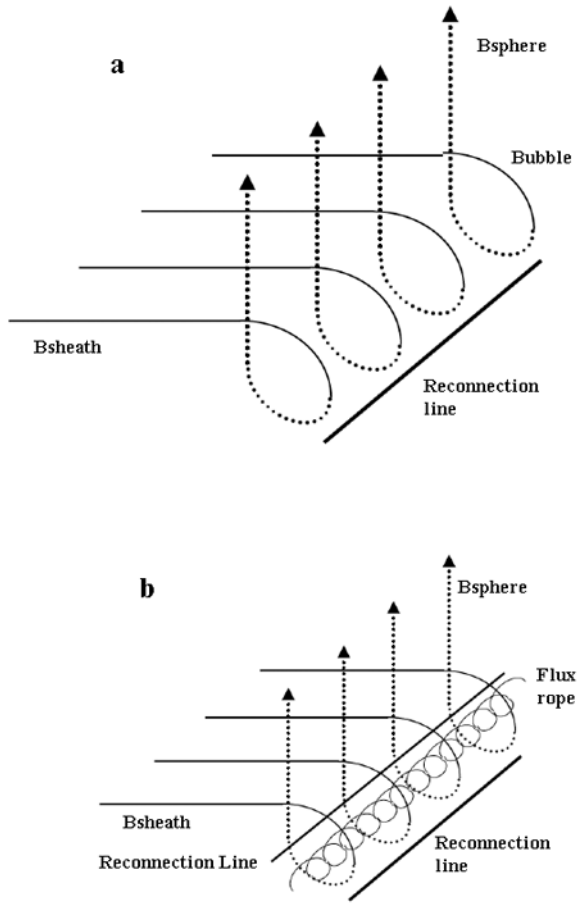

Figure 1. Two models for flux transfer event (FTE) formation along extended reconnection lines. (a) Single reconnection lines generate bulges of interconnected magnetosheath and magnetospheric magnetic field lines. (b) Multiple reconnection lines generate true flux ropes of twisted magnetic field lines surrounding an axial magnetic field.

test these and other hypotheses. Ideally, one might employ high-time and spatial resolution global magnetohydrodynamic or kinetic models to determine the conditions under which the events are generated and their characteristics for comparison with observations. Although FTEs have been seen in both global MHD [e.g., *Berchem et al.*, 1995; *Fedder et al.*, 2002; *Raeder*, 2006; *Sibeck et al.*, 2008] and 2.5-dimensional hybrid code models [*Omidi and Sibeck*, 2007], for the time being resource constraints and concerns about whether the models properly parameterize the fundamental physics that trigger reconnection preclude systematic studies employing multiple high-resolution runs to determine event occurrence patterns and characteristics as a function of solar wind conditions.

[5] Instead, we adopt a simpler approach. We assume that events are generated by near-instantaneous component reconnection along one or more extended lines passing through the immediate vicinity of the subsolar magnetopause with tilts dependent upon the IMF orientation. We employ the *Cooling et al.* [2001] model to determine the motion of the points where the magnetic field lines within these FTEs cross the magnetopause for a variety of IMF strengths and orientations, iteratively using this information to determine subsequent event orientations. We then use the components of the magnetic field and flow velocity perpendicular to the event axes to estimate the amplitudes of the plasma flow and magnetic field perturbations that the events generate in the ambient media. In particular, we show that events occurring for southward IMF orientations generate the largest perturbation signatures on the dayside equatorial magnetopause but are unlikely to reach the flanks. By contrast, events occurring for northward IMF orientations generate weak signatures on the dayside magnetopause but invariably move toward the flanks where their perturbation signatures can be greater than on the dayside magnetopause. Consequently events occurring for southward IMF orientations dominate surveys of FTEs on the dayside magnetopause but not on the flanks.

2. Method and Assumptions

[6] To determine the orientation and motion of FTEs, as well as the amplitudes of the perturbations they generate, we must make a series of assumptions concerning the motion of reconnected magnetic field lines, the nature of the magnetopause boundary, the characteristics of the ambient magnetosheath and magnetospheric plasmas and magnetic fields, the initial location and extent of the FTEs, and their dimensions perpendicular to the magnetopause boundary. In this section, we describe the reasons motivating these assumptions and note alternatives. At the end of the section, we summarize results from previous case and statistical studies employing similar assumptions to justify the assumptions.

[7] We assume that bursts of reconnection take place along single [*Southwood et al.*, 1988; *Scholer*, 1988] or multiple [*Lee and Fu*, 1985] reconnection curves, resulting in either bubbles of interconnected magnetosheath and magnetospheric magnetic field lines or true flux ropes, as illustrated respectively in Figures 1a and 1b. The curve (or curves) in Figures 1a and 1b have total lengths of 19 R_E, consistent with in situ observations of steady reconnection [*Phan et al.*, 2000, 2006], remote ground-based observations of signatures interpreted as FTEs [*Lockwood et al.*, 1990; *Milan et al.*, 2000; *Wild et al.*, 2003], and the predictions of global MHD simulations [*Fedder et al.*, 2002; *Raeder*, 2006; *Kuznetsova et al.*, 2009]. There are models in which patchy reconnection results in FTEs with much smaller dimensions [*Russell and Elphic*, 1978]. However, like *Fear et al.* [2008, 2009], we suspect that appropriate in situ observations will ultimately provide evidence for the frequent occurrence of FTEs with extents far greater than 1.5 R_E along the magnetopause. Nevertheless, we present our results in a format that enables readers to track the orientation and motion of FTEs with both large and small dimensions.

[8] We also assume that the bursts of reconnection transpire nearly simultaneously across the full extent of the reconnection curve. Bursts with durations far less than the 3 min mode and 8 min mean event recurrence rates [*Lockwood and Wild*, 1993] are implicit in the model for isolated transient FTEs proposed by *Lockwood et al.* [1990] and *Cowley and Lockwood* [1992]. In this model, the ionospheric boundary between open and closed magnetic field

lines abruptly jumps equatorward, and the entire region of newly reconnected magnetic field lines then moves poleward and antisunward into the polar cap. An alternative, not considered in this paper, is that the reconnection area might initially be localized but then propagate in a wave-like manner along the magnetopause for extended periods of time (10 min) and distances [*Saunders et al.*, 1992; *Milan et al.*, 2000; *Wild et al.*, 2003].

[9] Many models have been proposed for the location of the reconnection curves on the magnetopause. In this paper, we consider events produced along one or more component reconnection curves passing through the vicinity of the subsolar point on the magnetopause whose tilts depend upon the IMF orientation. Although the subsolar reconnection curve may assume any orientation between the sheared magnetosheath and magnetospheric magnetic fields [*Cowley*, 1976], we invoke component reconnection models that predict reconnection along curves that maximize the shear between magnetosheath and magnetospheric magnetic fields, that is, curves that parallel the magnetopause current vector [*Sonnerup*, 1974; *Gonzalez and Mozer*, 1974]. For duskward IMF orientations, the current vector runs from southern dawn to northern dusk across the dayside magnetopause, while for dawnward IMF orientations it runs from northern dawn to southern dusk. A reconnection curve with these tilts is consistent with particle anisotropy observations in the northern dawn quadrant indicating events connected to the northern ionosphere during periods of duskward IMF orientation, and events connected to the southern ionosphere during periods of dawnward IMF orientation [*Daly et al.*, 1984]. It is also consistent with simulation predictions [*Fedder et al.*, 2002; *Raeder*, 2006].

[10] In determining the current vector, we use the magnetosheath and magnetospheric magnetic field strengths and directions predicted by the *Kobel and Flückiger* [1994] and *Alexeev et al.* [2003] models at a paraboloid magnetopause for specified solar wind plasma and magnetic field conditions. The *Kobel and Flückiger* [1994] model defines magnetosheath magnetic fields as a function of the IMF components, the distance to the subsolar magnetopause (R_{SS}), and the distance to the subsolar bow shock (R_{BS}) from Earth, here taken to be $R_{BS} = 1.5\ R_{SS}$. The *Alexeev et al.* [2003] model specifies magnetospheric magnetic field strengths and directions within a paraboloid magnetopause as a function of dipole tilt, solar wind plasma density and velocity, IMF strength and direction, and geomagnetic indices *Dst* and *AL*. We set the dipole tilt equal to zero and *Dst* and *AL* = 0, corresponding to quiet times at the equinoxes. The model then sums contributions from Earth's dipole, superposed ("penetrated") IMF, ring, cross-tail, region 1, and Chapman-Ferraro currents to determine the total magnetic field strength and direction as a function of location within the dayside magnetosphere. In these models, the subsolar point is given by [*Shue et al.*, 1997]

$$R_{SS} = (11.4 + 0.013B_Z)p_{SW}^{-1./6.6} \text{ for IMF } B_Z > 0$$

and

$$R_{SS} = (11.4 + 0.14B_Z)p_{SW}^{-1./6.6} \text{ for IMF } B_Z < 0,$$

where R_{SS} is in Earth radii (R_E), B_Z is the north/south component of the IMF (in nT), and p_{SW} is the solar wind dynamic pressure (in nPa). The terminator lies at a distance of $2^{0.5}\ R_{SS}$ from Earth.

[11] Other component reconnection models predict reconnection along the locus of points where magnetosheath magnetic field lines first contact the magnetopause [*Crooker et al.*, 1990], along curves of maximum shear that lie far from the equator in the winter hemisphere [*Trattner et al.*, 2007], or along the locus of points that maximizes the Alfvén speed characterizing the reconnection outflow [*Swisdak and Drake*, 2007]. Nevertheless, all these component reconnection models share a common prediction that the inclination of the dayside reconnection curve out of the plane of the geomagnetic equator increases as the orientation of the IMF rotates from due southward to strongly northward.

[12] The very different predictions of the antiparallel or split separator reconnection models lie outside the scope of this paper. These models predict reconnection curves that lie along the locus of points where magnetosheath and magnetospheric magnetic fields point in (nearly) opposite directions [*Crooker*, 1979]. For duskward (dawnward) IMF orientations, reconnection ceases on the equatorial magnetopause and moves to the high-latitude northern dusk (dawn) and southern dawn (dusk) quadrants [*Luhmann et al.*, 1984]. For strongly southward IMF orientations, the length of the curves diminishes when Earth's dipole tilts sunward or antisunward [*Russell et al.*, 2003]. In particular, reconnection ceases in the vicinity of local noon for all but due southward IMF orientations. The split separator line model predicts the formation of FTEs on the dayside equatorial magnetopause between split reconnection curves passing through the cusps at high latitudes [*Crooker*, 1985]. Perhaps the distinction between component and antiparallel reconnection models is overemphasized. Simulations [*Dorelli et al.*, 2007] and observations [*Fuselier et al.*, 2000; *Trattner et al.*, 2004] indicate that both can operate simultaneously.

[13] The point at which any given reconnected field line intersects the magnetopause surface moves with the local de Hoffman-Teller frame velocity. As described by *Cowley and Owen* [1989] and *Cooling et al.* [2001], the plasma velocity in the de Hoffman-Teller frame is given by the Alfvén velocity either parallel or antiparallel to the magnetic field. The de Hoffman-Teller velocity is then given by the sum of the local magnetosheath flow velocity and the Alfvén velocity in the magnetosheath, with the sense of flux tube connection to the magnetosphere (Northern Hemisphere or Southern Hemisphere) determining the sign of the Alfvén velocity (antiparallel or parallel to the draped magnetosheath magnetic field).

[14] Because they consist solely of magnetic field lines that cross the magnetopause locally, the reconnected magnetic field lines in bubbles move in the direction and at the speed predicted by the *Cooling et al.* [2001] model from the moment of their inception along single reconnection lines. By contrast, flux ropes form between pairs of reconnection lines and may initially lie nearly stationary on the magnetopause until such time as an imbalance in forces causes them to begin moving. We assume that the more recently reconnected magnetic field lines that loop over the flux ropes then accelerate them to the velocities predicted by the

Cooling et al. [2001] model. If the forces do not do so, then the flux ropes will move at speeds less than those predicted by the model.

[15] To determine the velocities of the points in the FTEs, we need magnetosheath magnetic fields, densities, and velocities just outside the magnetopause. *Kobel and Flückiger* [1994] provide the magnetosheath magnetic fields, while *Cooling et al.* [2001] provide magnetosheath densities and velocities obtained from fits to the *Spreiter et al.* [1966] gasdynamic model results just outside the magnetopause for a fast magnetosonic Mach number of 8 and an adiabatic index γ of 5/3. In the Spreiter et al. model, the magnetopause lies along the locus of points where magnetospheric magnetic pressures balance gasdynamic magnetosheath plasma pressures determined from the Newtonian approximation. As noted by *Kobel and Flückiger* [1994], the similarity of the draped magnetosheath magnetic field line patterns for radial and transverse IMF orientations in the Kobel-Flückiger and Spreiter et al. models suggests that their use in tandem is justified despite the differing shapes for the magnetopause in the two models. These simple models for magnetosheath plasma and magnetic field parameters may require modification during periods when the IMF has a northward orientation and magnetohydrodynamic effects cause a depletion layer of enhanced magnetic field strengths and depressed densities to form just upstream from the dayside magnetopause [*Crooker et al.*, 1979]. When a depletion layer is present, magnetosheath Alfvén velocities increases, and magnetic curvature forces play a more significant role in determine the direction of event motion. We will consider the effects of a depletion layer by presenting two IMF B_y case studies with identical magnetosheath magnetic field orientations but different magnetic field strengths.

[16] We move individual points in the events with the velocities appropriate to their location and then connect these points to determine the location, length, and orientation of the events at subsequent times. In doing this, we ignore the possibility that kink or other mode instabilities might introduce additional velocities and distort event orientations. Such instabilities would be most likely for events with weak axial and strong poloidal magnetic fields, as might be expected during intervals of due southward IMF when reconnection between nearly antiparallel magnetosheath and magnetospheric magnetic fields occurs along the equator. We also ignore the effects of magnetosheath turbulence, which would introduce irregularities into the speeds at which different portions of the event move and result in events with bent axes.

[17] As the events move along the surface of the paraboloid magnetopause, they displace the surrounding media, generating plasma and magnetic field signatures [*Cowley*, 1982; *Farrugia et al.*, 1988; *Sibeck et al.*, 2005; *Sibeck*, 2009; *Korotova et al.*, 2009]. When there is a difference between ambient media and event velocities in the direction perpendicular to the event axis, the passage of an event generates not only a reverse flow in the direction perpendicular to the event axis, but also a bipolar flow normal to the nominal magnetopause surface. The reverse flow perturbations peak on the surface of the event in a plane parallel to the nominal magnetopause at the points of maximum protrusion into the magnetosheath and magnetosphere, while the flow perturbations normal to the nominal magnetopause peak on the surface of the event at locations that depend upon the shape of the event but lie between the point of maximum protrusion and the intersection of the event with the magnetopause. The amplitudes of the bipolar perturbations normal to the nominal magnetopause exceed those for the compressional component in the plane parallel to the magnetopause when the distance that an event with an elliptical cross section protrudes into the neighboring regions is less than its half width along the magnetopause but are less than those for the compressional component for events in which the distance that the event protrudes into the neighboring regions exceeds the half width along the magnetopause. Events moving faster than the ambient magnetosheath flow generate outward/inward flow perturbations in the magnetosheath but inward/outward flow perturbations in the otherwise stagnant magnetosphere. Greater flow differentials result in greater flow perturbations.

[18] Similarly, when there is a component of the ambient magnetic field perpendicular to an event's axis, the passage of an FTE generates not only an enhancement in the magnetic field strength, but also a bipolar magnetic field component normal to the nominal magnetopause. When there is a component of event motion parallel to the magnetic field, the sense of the bipolar perturbation is inward/outward ("reverse signature") in the magnetosheath but outward/inward ("direct signature") in the magnetosphere. The senses reverse when the event moves antiparallel to the magnetic field, and the amplitude of the perturbations increases for larger magnetic field components transverse to the event axis. The components of the perturbation magnetic field in and perpendicular to the nominal magnetopause peak in the same locations as those for the perturbation flow velocities.

[19] We will therefore use the components of the event speed relative to the background flow and the ambient magnetic field perpendicular to the event axes as indicators of the amplitudes of the perturbations generated in the ambient media. However, to compare event amplitudes in the magnetosheath and magnetosphere at various locations on the magnetopause for differing solar wind conditions, we must also take into account the fact that perturbation amplitudes also depend upon event dimensions. Although we assume identical event widths (or burst durations) for all the cases considered in this paper, we cannot assume identical event dimensions normal to the magnetopause. Greater magnetic curvature forces in the magnetosphere than in the magnetosheath displace events outward, resulting in larger perturbation signatures in the magnetosheath than the magnetosphere [*Ding et al.*, 1991]. *Sibeck* [2009] balanced curvature forces in the magnetosheath and magnetosphere to derive an analytical solution for the distance b_1 that an event with a circular magnetosheath cross section of radius a protrudes into the magnetosphere as a function of the magnetic field strengths and orientations in both regions: $b_1 = 0.5a\{1 + 8(\cos\theta - B_2/B_1)^2/(B_1/B_2 - \cos\theta)^2]^{1/2} - 1\}$, where $\mathbf{B_1}$ and $\mathbf{B_2}$ are the local magnetosphere and magnetosheath magnetic fields predicted by the *Alexeev et al.* [2003] and *Kobel and Flückiger* [1994] models and $\cos\theta = \mathbf{B_1} * \mathbf{B_2}/|\mathbf{B_1}||\mathbf{B_2}|$. While we take the full values of the flow velocity differential and magnetic field strength

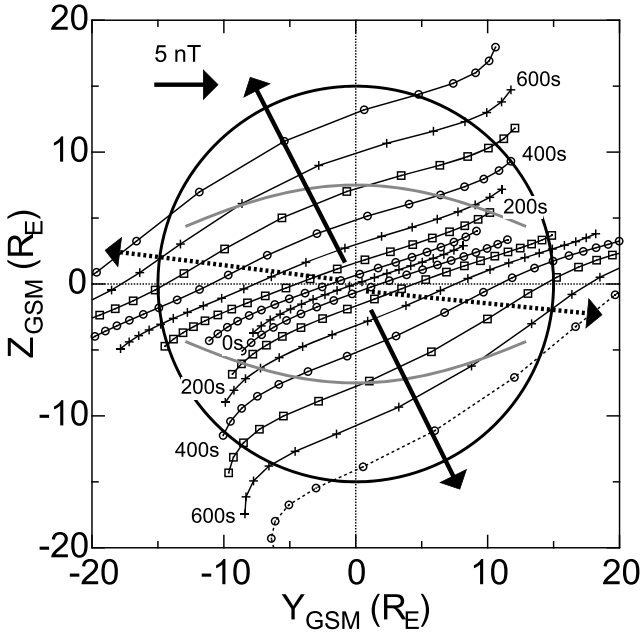

Figure 2. FTE motion away from a tilted subsolar component reconnection curve for a 5 nT duskward interplanetary magnetic field (IMF), solar wind density of 5 cm^{-3}, and solar wind velocity of 400 km s^{-1}. Events connected to the northern and southern hemispheres are shown each 100 s. Crosses, circles, and squares on the events show the locations of points originally separated by 1 R_E. Dashed arrows indicate the dawnward motion of equatorial fluid parcels connected to the Northern Hemisphere and duskward motion of equatorial fluid parcels connected to the Southern Hemisphere. These are the plasma velocities that would be observed by a spacecraft entering the events. Solid arrows indicate the component of these velocities transverse to event axes. These are the velocities that would be determined from timing studies. Gray curves illustrate two magnetosheath magnetic field lines draped against the magnetopause. The solid circle in this and subsequent figures represents the terminator on the magnetopause at $X = 0$.

perpendicular to the event axes as a measure of the perturbations generated in the magnetosheath, to account for the shallower cross sections in the magnetosphere we normalize (invariably diminishing) the components of the magnetospheric flow differentials and magnetic field strengths perpendicular to the event axes by a factor of b_1/a (<1).

[20] Given the many assumptions invoked above, it may come as a surprise that the model ever predicts event motion accurately. Yet several case studies have employed the *Cooling et al.* [2001] model to trace the motion of events backward in time and have confirmed that they could have originated along reconnection lines with the tilts and locations expected for the prevailing solar wind conditions [*Fear et al.*, 2005; *Dunlop et al.*, 2005; *Wild et al.*, 2005, 2007]. More recently, *Fear et al.* [2007] reported that FTE velocities inferred from timing considerations and multipoint in situ Cluster observations were consistent with Cooling et al. model predictions for the motion of reconnected magnetic field lines in 78% of 118 cases, where consistency demanded that observed velocities lie within 30° of those predicted and observed speeds lie within a factor of 2 of those predicted for open field lines connected to either the northern or southern ionosphere (i.e., north or south from the reconnection line).

[21] Inspired by these successes but sobered by the numerous assumptions required, we will employ the *Cooling et al.* [2001] model to predict the motion of FTEs generated by component reconnection along tilted subsolar curves for a variety of IMF orientations. We will then determine the plasma flow and magnetic field perturbations generated by these events in the ambient media.

3. Event Motion, Orientation, and Signatures

[22] In this section, we consider sequentially the motion and perturbation signatures of FTEs for (1) a weak duskward IMF, (2) a strong duskward IMF, (3) an away sector IMF lying along the Parker spiral, (4) a southward IMF, and (5) a northward and duskward IMF.

3.1. Weak Duskward Interplanetary Magnetic Field (IMF)

[23] Consider the motion of FTEs for a solar wind density of 5 cm^{-3} and velocity of 400 km s^{-1} and a weak 5 nT duskward IMF B_y. As indicated by the two gray curves in Figure 2, draped magnetosheath magnetic field lines bow poleward. In this and every other case to be considered, magnetospheric magnetic field lines bow dawnward prior to local noon and duskward after local noon (not shown). For these magnetosheath and magnetospheric magnetic field orientations, the component reconnection model predicts reconnection and therefore FTE generation along a slightly inclined reconnection curve passing from southern dawn to northern dusk through the subsolar point. This curve is labeled 0s in Figure 2. We set the length of the curve to 19 R_E, with 9.5 R_E on either side of local noon, and mark off crosses each 1 R_E.

[24] We track the motion of these points and connect their loci to determine the location and orientation of FTEs on magnetic field lines connected to the northern and southern hemispheres at subsequent intervals separated by 100 s. Magnetic curvature forces pull points connected to the northern ionosphere dawnward but points connected to the Southern Hemisphere duskward, while pressure gradient forces push points radially antisunward from the subsolar point. As illustrated by the large dashed arrows in Figure 2, equatorial points move either dawnward or duskward in response to the combined magnetic curvature and pressure gradient forces. However, it is the component of this motion perpendicular to the event axes that causes events to move past observing spacecraft. Consequently, as illustrated by the large solid arrows in Figure 2, events north of the reconnection line appear to move northward and dawnward, while events south of the reconnection line appear to move duskward and southward. These are the (very different) velocities that would be deduced from multipoint spacecraft timing studies. Note that the FTEs retain the original southern-dawn to northern-dusk orientation of the reconnection line and require more than 700 s to clear the dayside magnetopause as they slowly accelerate antisunward.

[25] We take the components of the ambient magnetic fields perpendicular to event axes at each point on those

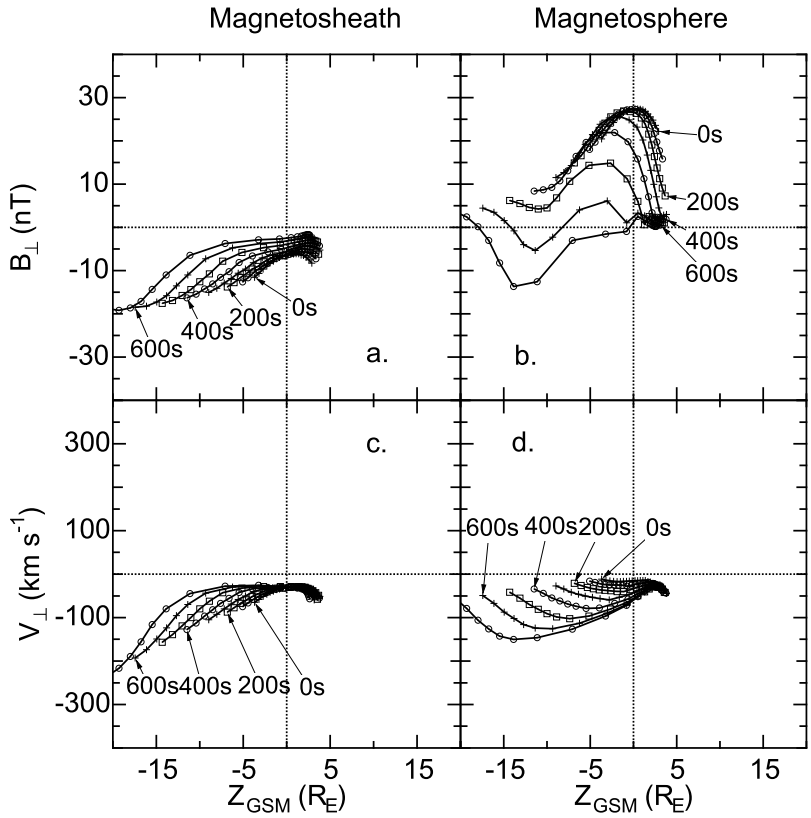

Figure 3. Components of the (a) magnetosheath magnetic field, (b) normalized magnetospheric magnetic field, (c) shear between magnetosheath and event velocities, and (d) normalized shear between magnetospheric and event velocities perpendicular to the event axis as a function of time and distance from the equatorial plane for the 5 nT duskward IMF case shown in Figure 2. Magnetospheric values are normalized by balancing magnetosheath and magnetospheric curvature forces to reduce the distances that events with circular magnetosheath cross sections protrude into the magnetosphere and therefore the amplitudes of the perturbations that they produce in the magnetosphere. Values are shown for events connected to the Southern Hemisphere at each of the points and each of the times illustrated in Figure 2.

axes as measures of the perturbations that the events produce in the surrounding media. We obtain these components by calculating (**n** × **A**) * **B** at each point on the event, where **n** is the unit normal to the magnetopause, **A** is a unit vector along the event axis running from dawn to dusk, and **B** is the ambient magnetic field obtained from either the *Kobel and Flückiger* [1994] or *Alexeev et al.* [2003] model. Figure 3a shows this component at each point on the southward and duskward moving FTE in the magnetosheath as a function of time and distance from the equatorial plane. Event "amplitudes" are greater off the equator (~15 nT) than at the equator (~5 nT) at each instant but diminish with time at fixed distances south of the equator as the event moves into regions where the magnetosheath magnetic field lies less perpendicular to the event axis. Because there is a component of the event's motion parallel to the direction of the magnetosheath magnetic field, the southward moving event generates "reverse" bipolar in/out magnetic field signatures normal to the nominal magnetopause in the magnetosheath. By symmetry, the signatures for northward moving events can be obtained by reflecting the traces about the $Z = 0$ axis. The latter events move antiparallel to the magnetosheath magnetic field and therefore generate "direct" bipolar out/in magnetic field signatures normal to the nominal magnetopause in the magnetosheath.

[26] Figure 3b presents corresponding information for the "normalized" component of the magnetospheric magnetic field perpendicular to the event axis. As the event moves southward/duskward and encounters weaker magnetospheric magnetic field strengths, the component of the (northward) magnetospheric magnetic field strength perpendicular to its axis steadily decreases from 25 to 0 nT. Eventually portions of the event reach locations poleward of the southern cusp at $Z = -10\ R_E$, where negative perturbations (−15 nT) indicate encounters with southward pointing lobe magnetic field lines. Because there is a component of event motion opposite the direction of the magnetospheric magnetic field, the event generates "reverse" bipolar in/out magnetic field signatures normal to the nominal magnetopause in the dayside magnetosphere. The event generates "direct" bipolar out/in signatures poleward of the southern cusp. By symmetry, the signatures for northward moving events can be obtained by reflecting the traces about the $Z = 0$ axis. Northward moving events generate "direct" bipolar magnetic field signatures normal to the nominal magnetopause on the dayside magnetosphere but "reverse" signatures

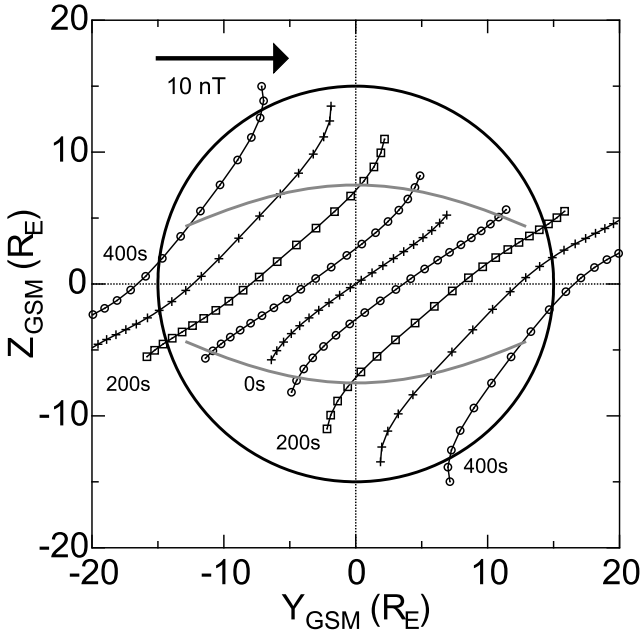

Figure 4. FTE motion away from a tilted subsolar component reconnection curve for a 10 nT duskward IMF, solar wind density of 5 cm^{-3}, and solar wind velocity of 400 km s^{-1}. Events connected to the northern and southern hemispheres are shown each 100 s. Crosses, circles, and squares on the events show the locations of points originally separated by 1 R_E. Gray curves illustrate two magnetosheath magnetic field lines draped against the magnetopause.

poleward of the northern cusp. As perturbation amplitudes in the equatorial magnetosphere (Figure 3b) are far greater than those in the equatorial magnetosheath (Figure 3a), equatorial spacecraft should record more events in the magnetosphere than in the magnetosheath. By contrast, similar amplitudes imply similar occurrence rates off the equator.

[27] We take the component of the difference between the event ($\mathbf{V_{event}}$) and ambient ($\mathbf{V_{ambient}}$) velocities perpendicular to the event axis as a measure of the flow perturbation that the event produces in the ambient media. We calculate this component at each point on the events as $(\mathbf{n} \times \mathbf{A}) * (\mathbf{V_{event}} - \mathbf{V_{ambient}})$. We set $\mathbf{V_{ambient}}$ to 0 in the magnetosphere and the magnetosheath velocity just outside the magnetopause in the magnetosheath. Figure 3c shows this component of the flow differential in the magnetosheath at each point on the southward/duskward moving FTE as a function of time and distance from the equatorial plane. The flow differential remains small (~50 km s^{-1}) in the vicinity of the equator but attains greater values further from the equator in the prenoon sector where the draped magnetosheath magnetic field lies more nearly perpendicular to the axis of the accelerating event. As the event moves duskward into regions where the draped magnetosheath magnetic field strength lies more nearly parallel than perpendicular to the event axis, the tug on the FTE relative to the magnetosheath flow diminishes steadily. By symmetry, the velocity perturbations for the event moving northward and dawnward can be obtained by mirroring those shown in Figure 3c about both the $V_\perp$ and Z axes. Because the events move through the magnetosheath flow at speeds faster than that flow, they generate weak outward/inward bipolar flow signatures normal to the nominal magnetopause in the magnetosheath.

[28] Figure 3d shows the normalized component of the flow differential perpendicular to the axis of the event in the magnetosphere. Flow differentials remain small near the geomagnetic equator but increase rapidly at more southerly locations as the event accelerates. Symmetry requires signatures north of the equator to be a reflection of those shown in Figure 3d about both axes. In both cases, the events generate inward/outward flow signatures in the stagnant magnetospheric plasma.

3.2. Strong Duskward IMF

[29] Next we consider the motion of FTEs for a solar wind density of 5 cm^{-3} and velocity of 400 km s^{-1} and a strong 10 nT duskward IMF B_y. This scenario corresponds either to a greater IMF strength than that studied in section 3.1 or the presence of a depletion layer with enhanced magnetic field strengths. As indicated by the gray curves in Figure 4, magnetosheath magnetic field lines again bow poleward. Thanks to enhanced magnetosheath magnetic field strengths, the tilt of the subsolar reconnection line along which events form at "0 s" away from the equator is greater than that for the IMF B_y = 5 nT case. The events depart the dayside magnetopause in just over 400 s, indicating that the enhanced magnetic curvature forces associated with larger magnetosheath magnetic field strengths remove the events from the dayside magnetopause much more rapidly than in the IMF B_y = 5 nT case. Although the events retain orientations similar to those of the reconnection line, less time is available for stretching by pressure gradient forces, and the events do not attain the lengths seen in the previous case. A comparison of Figures 3 and 5 demonstrates that magnetosheath magnetic field perturbations are (as expected) about twice as great as they were for the IMF B_y = 5 nT case, but that the enhanced magnetosheath magnetic field strengths have little effect on the amplitudes of the magnetic field perturbations in the magnetosphere. As in the previous case, magnetosheath magnetic field perturbations diminish with time at fixed distances from the equator. Events moving southward generate bipolar in/out signatures in the magnetosheath and magnetospheric magnetic fields, while those moving northward generate bipolar out/in signatures.

[30] Velocity perturbations are substantially greater for the IMF B_y = 10 nT case than for the IMF B_y = 5 nT case, particularly in the magnetosheath due to the greater magnetic curvature forces there. Because they move faster than the background flows in the magnetosheath and magnetosphere, the events generate outward/inward flow signatures in the magnetosheath but inward/outward flow signatures in the magnetosphere.

3.3. Duskward Spiral IMF Orientation

[31] The IMF typically points neither duskward nor dawnward, but rather inward or outward along the Parker spiral. In this section, we consider the motion and signatures of FTEs generated by component reconnection for a solar wind density of 5 cm^{-3} and velocity of 400 km s^{-1} and a strong outward pointing Parker spiral IMF with IMF $B_y = -B_x$ = 7.07 nT. For this IMF orientation, draped magne-

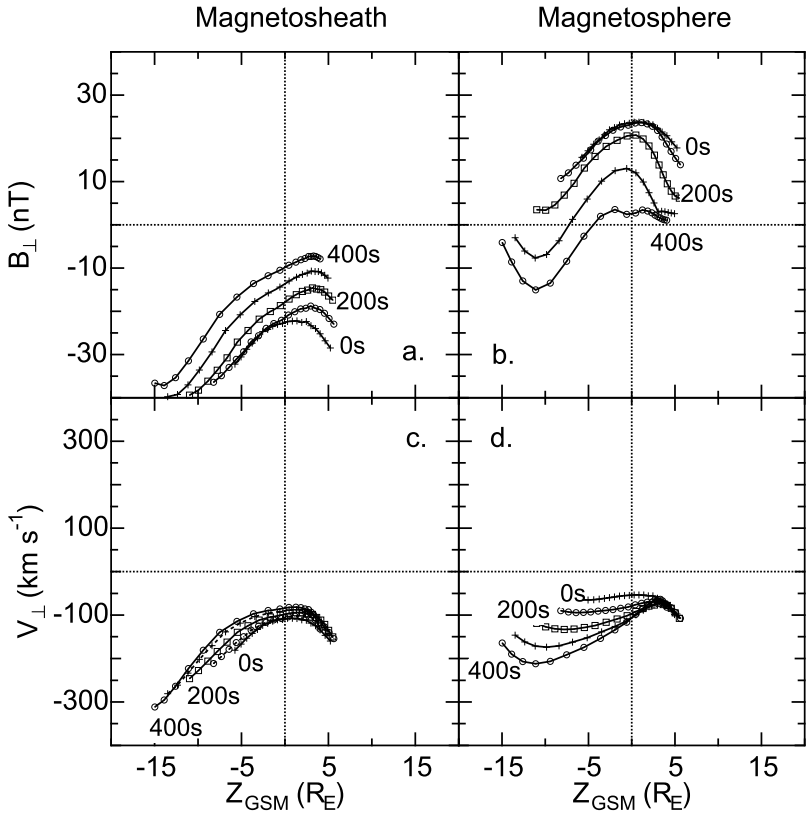

Figure 5. Components of the (a) magnetosheath magnetic field, (b) normalized magnetospheric magnetic field, (c) shear between magnetosheath and event velocities, and (d) normalized shear between magnetospheric and event velocities perpendicular to the event axis as a function of time and distance from the equatorial plane for the 10 nT duskward IMF case shown in Figure 4. Magnetospheric values are normalized by balancing magnetosheath and magnetospheric curvature forces to reduce the distances that events with circular magnetosheath cross sections protrude into the magnetosphere. Values are shown for events connected to the Southern Hemisphere at each of the points and each of the times illustrated in Figure 4.

tosheath magnetic field lines diverge from a point on the prenoon equatorial magnetopause, as illustrated by the gray curves in Figure 6. The southern/dawn to northern/dusk tilt of the subsolar reconnection line along which events form at "0 s" is similar to that for the strong duskward IMF case. The FTEs preserve this orientation as they depart the dayside magnetopause, moving more rapidly southward and duskward than northward and dawnward because the strength of the magnetosheath magnetic field draped against the postnoon magnetopause is greater than that splayed against the prenoon magnetopause.

[32] The signatures generated by the events in the surrounding media are no longer symmetric about the equatorial and noon meridian planes. Figure 7 shows the signatures generated by the events moving dawnward and northward. In the vicinity of the equator, both magnetosheath and magnetospheric magnetic field perturbations decrease steadily as the event moves dawnward, with perturbation amplitudes in the magnetosphere (<25 nT) greater than those in the magnetosheath (<15 nT). Because there is a component of motion parallel to the magnetospheric magnetic field but opposite the magnetosheath magnetic field, the dawnward/northward moving events generate bipolar out/in signatures in the magnetosphere and magnetosheath. In the vicinity of the equator, magnetosheath flow perturbations diminish with distance from the point of origin as the curvature force (which moves events relative to the magnetosheath flow) diminishes. By contrast, magnetospheric flow perturbations increase slightly as the increase in event velocity resulting from pressure gradient acceleration exceeds the decrease resulting from diminishing magnetic curvature forces. Both velocities remain relatively small at the equator, <100 km s^{-1}, due to the slow speed of the prenoon events. Because they move faster than the background flows, the events generate in/out flow signatures in the magnetosphere but out/in flow signatures in the magnetosheath.

[33] Figure 8 presents the signatures generated by events moving duskward and southward. Magnetosheath magnetic field perturbation amplitudes increase with distance southward from the equator but remain relatively constant with time at fixed distances from the equator. By contrast, magnetosheath magnetic field perturbation amplitudes diminish rapidly with time at fixed distances north of the equator. As a result, the amplitudes that the events generate in the magnetosheath diminish toward dusk at fixed distances north of the magnetopause but remain nearly constant toward dusk at fixed distances south of the equator. Perturbation amplitudes in the magnetosphere peak near the

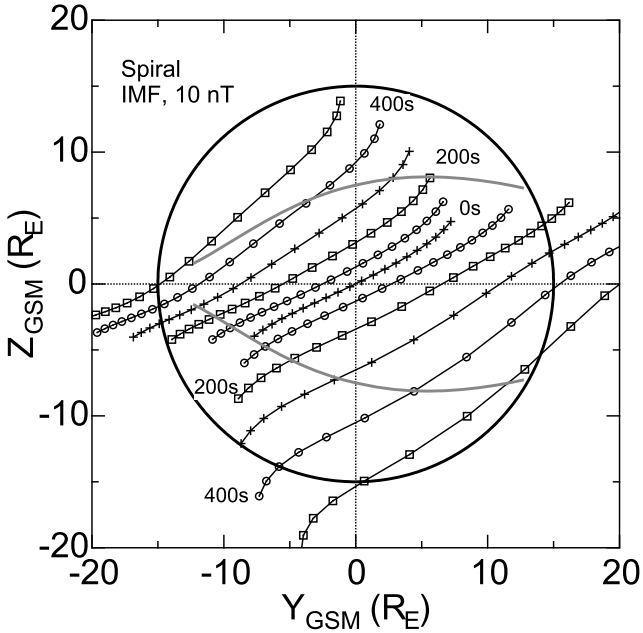

Figure 6. FTE motion away from a tilted subsolar component reconnection curve for a 10 nT spiral IMF with $B_y = -B_x = 7.1$ nT, solar wind density 5 cm^{-3}, and solar wind velocity 400 km s^{-1}. Events connected to the northern and southern hemispheres are shown each 100 s. Crosses, circles, and squares on the events show the locations of points originally separated by 1 R_E. Gray curves illustrate two magnetosheath magnetic field lines draped against the magnetopause.

equator but diminish rapidly with time and/or distance from the equator. Because there is a component of motion parallel to magnetosheath magnetic fields but antiparallel to magnetospheric magnetic fields, the southward/duskward moving events generate in/out magnetic field perturbations in both regions. Magnetosheath flow perturbations pass through a minimum at the equator, increase to 300 km s^{-1} off the equator, and remain relatively constant at fixed distance from the equator throughout the event's motion, while those in the magnetosphere increase steadily to values as great as 200 km s^{-1} with distance south from the equator and with time at fixed distances south of the equator. Because the events move through the magnetosheath at flows faster than those of the magnetosheath itself, they generate out/in flow perturbations in the magnetosheath but in/out flow perturbations in the magnetosphere.

3.4. Due Southward IMF Orientations

[34] Numerous studies indicate that the chance of observing an FTE on the dayside magnetopause is greatest for southward IMF orientations [e.g., *Berchem and Russell*, 1984; *Kuo et al.*, 1995]. We now consider the motion of an FTE for a solar wind density of 5 cm^{-3} and velocity of 400 km s^{-1} and a 10 nT southward IMF B_z. As illustrated by the gray curves in Figure 9, the draped magnetosheath magnetic field lines bow toward the flanks. The component reconnection model predicts reconnection and therefore FTE generation along the equatorial reconnection curve labeled 0s. Curvature forces associated with the draped magnetosheath magnetic field lines cause the poleward moving FTEs to bow equatorward. Nevertheless, because points on the FTE within ~5 R_E of the noon meridian ($Y = 0$ R_E) move poleward at similar velocities, the portion of the event near local noon retains an east-west orientation similar to that of the reconnection line. The motion of individual points on the FTE (large dashed arrow) and the component of this velocity that would be determined from timing studies (large solid arrow) are nearly identical. The events ultimately slip over the polar magnetopause, never reaching the equatorial flanks of the magnetosphere.

[35] Figure 10a shows the component of the magnetosheath magnetic field perpendicular to the event axis at each point on the southward moving FTE as a function of time and distance from the equatorial plane. As the event enters regions of weaker magnetosheath magnetic field strength, the amplitudes of the perturbations that it generates steadily diminish, as does the likelihood of it being detected. Perturbation amplitudes are slightly greater near noon than they are toward the flanks at each time and reach large values, 40 nT, at the equator. Because the southward moving event moves parallel to the direction of the magnetosheath magnetic field, it generates "reverse" bipolar in/out magnetic field signatures normal to the nominal magnetopause in the magnetosheath. Northward moving events generate "direct" bipolar out/in magnetic field signatures normal to the nominal magnetopause in the magnetosheath.

[36] Figure 10b presents corresponding information for the normalized component of the magnetospheric magnetic field perpendicular to the event axis. As the event moves southward, the component of the (northward) magnetospheric magnetic field strength perpendicular to its axis decreases, passes through zero at the cusp near $Z = -10$ R_E, turns southward, and becomes increasingly stronger. The perturbations generated by the event in the magnetosphere therefore diminish as it moves poleward toward the cusp but then increase as it moves poleward beyond the cusp. The perturbations are greatest near local noon (where magnetospheric magnetic field strengths are greatest) and diminish toward both dawn and dusk. They reach large values, 40 nT, at the subsolar point. Because the southward moving event moves opposite the direction of the magnetospheric magnetic field at latitudes below the cusp but parallel to the magnetospheric magnetic field at latitudes poleward of the cusp, it generates "reverse" inward/outward bipolar magnetic field signatures normal to the nominal magnetopause on the dayside magnetopause but "direct" outward/inward bipolar magnetic field signatures poleward of the southern cusp. The sense of the bipolar magnetic field signatures normal to the nominal magnetopause in each region reverses for northward moving events connected to the Northern Hemisphere.

[37] We take the component of the difference between the event and ambient velocities perpendicular to the event axis as a measure of the flow perturbation that the event produces in the ambient media. Figure 10c shows this component of the flow differential in the magnetosheath at each point on the FTE as a function of time and distance from the equatorial plane. Because both the event orientation and the Alfvén velocity within the inner magnetosheath remain relatively constant across the face of the dayside magnetopause, the flow perturbation also remains relatively constant

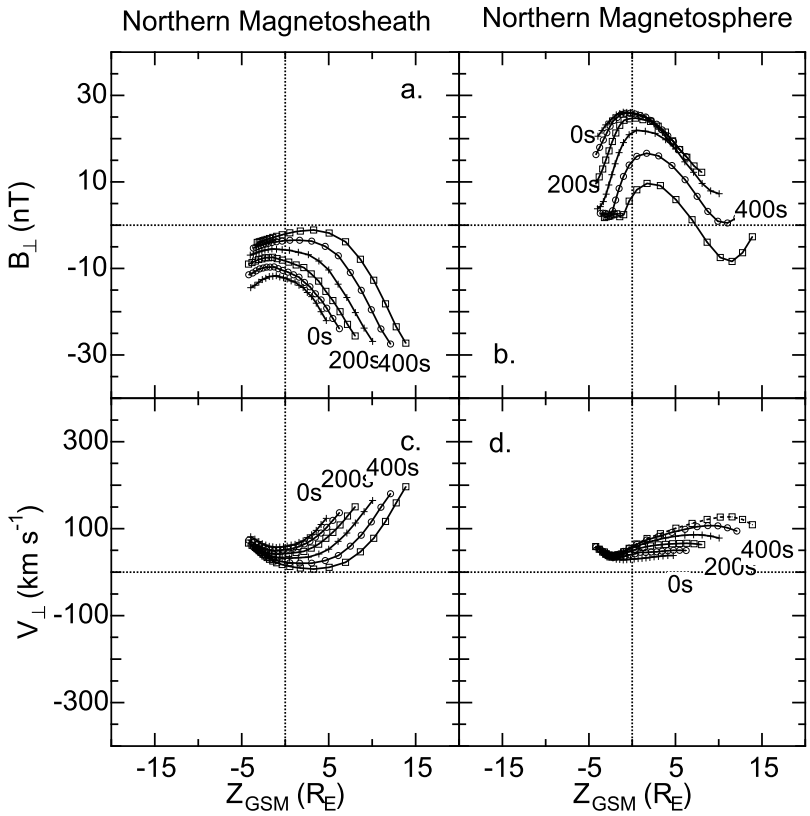

Figure 7. Components of the (a) magnetosheath magnetic field, (b) normalized magnetospheric magnetic field, (c) shear between magnetosheath and event velocities, and (d) normalized shear between magnetospheric and event velocities perpendicular to the event axis as a function of time and distance from the equatorial plane for the event connected to the Northern Hemisphere in the spiral IMF case shown in Figure 6. Magnetospheric values are normalized by balancing magnetosheath and magnetospheric curvature forces to reduce the distances that events with circular magnetosheath cross sections protrude into the magnetosphere. Values are shown for events connected to the Southern Hemisphere at each of the points and each of the times illustrated in Figure 6.

at 200–300 km s^{-1} as the event moves poleward. Peak perturbations occur at the dawn and dusk extremities of the event, where Alfvén velocities are slightly greater due to lower densities on the flanks. Because the events move through the magnetosheath flow in the same direction of the flow but at speeds faster than that flow, they generate outward/inward bipolar flow signatures normal to the nominal magnetopause in the magnetosheath.

[38] Figure 10d shows the normalized component of the flow differential perpendicular to the axis of the event in the magnetosphere. This component increases steadily on the noon meridian as the event moves poleward but eventually diminishes at the dawn and dusk extremities of the event because points on the extremities of the event begin to move parallel, rather than perpendicular, to its axis as the event bows equatorward. The event generates inward/outward flow perturbations in the magnetosphere.

3.5. Northward and Duskward IMF Orientations

[39] Finally, consider the motion and signatures of FTEs for a solar wind density of 5 cm^{-3} and velocity of 400 km s^{-1} and an IMF that points northward and duskward (IMF $B_y = B_z = 7.07$ nT). As indicated by the gray curves in Figure 11, the draped magnetosheath magnetic field lines bow toward the northern dawn and southern dusk flanks. The greatly inclined subsolar component reconnection curve again tilts from southern dawn to northern dusk. Combined pressure gradient and magnetic curvature forces have larger components along event axes than perpendicular to them and therefore stretch events both northward and southward as they are pulled dawnward or duskward, depending on their connection to the northern or southern magnetosphere. The large dashed arrow shows the northward and duskward motion of a field line within the FTE connected to the Southern Hemisphere from its initial location on the subsolar reconnection line to its final location on the northern dusk flank. FTE timing studies can only determine the component of this velocity normal to event axes. As indicated by the large solid arrow, this component points duskward and slightly southward. Despite the acceleration manifested by the increasing spacing between event snapshot locations, the events move far more slowly than those during southward IMF shown in Figure 9. Events occurring for northward and duskward IMF orientations require at least 500 s to transit the dayside magnetopause, as compared to 300 s for the southward IMF event.

[40] Figure 12a shows the magnetosheath magnetic field component perpendicular to the axes of the duskward

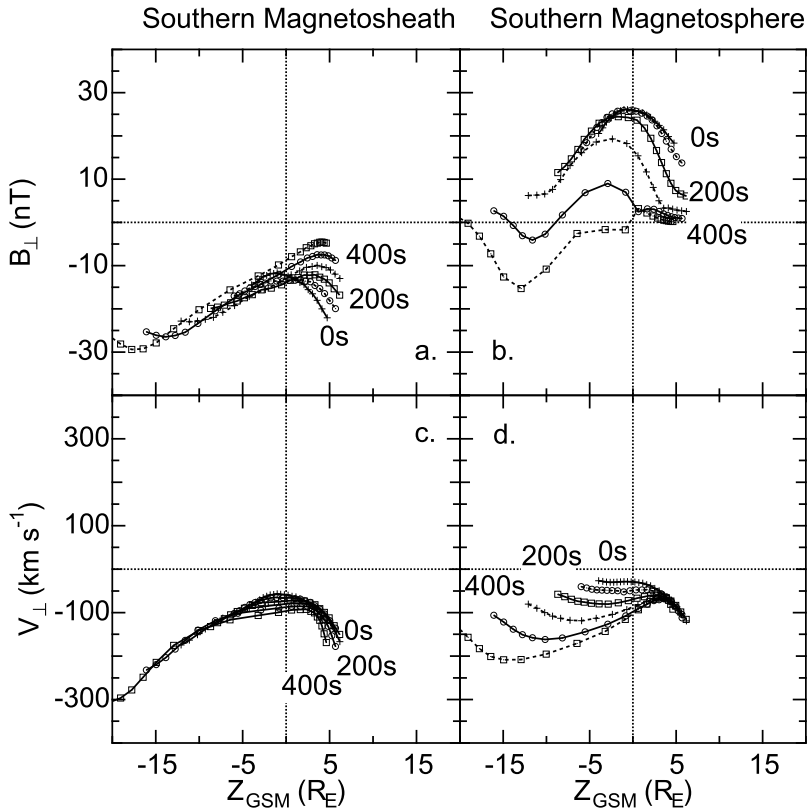

Figure 8. Components of the (a) magnetosheath magnetic field, (b) normalized magnetospheric magnetic field, (c) shear between magnetosheath and event velocities, and (d) normalized shear between magnetospheric and event velocities perpendicular to the event axis as a function of time and distance from the equatorial plane for the event connected to the Southern Hemisphere in the spiral IMF case shown in Figure 6. Magnetospheric values are normalized by balancing magnetosheath and magnetospheric curvature forces to reduce the distances that events with circular magnetosheath cross sections protrude into the magnetosphere. Values are shown for events connected to the Southern Hemisphere at each of the points and each of the times illustrated in Figure 6.

moving event as a function of time and distance from the equatorial plane. Initially this component is nearly constant at −15 nT across the entire length of the event. As the event moves, the magnitude of this component increases rapidly in the Southern Hemisphere where the angle between the event axis and the magnetosheath magnetic field increases, remains constant at the equator, but diminishes in the Northern Hemisphere. As there is a component of event motion parallel to the magnetosheath magnetic field, the duskward moving event generates in/out bipolar magnetic field signatures normal to the nominal magnetopause in both magnetosheath hemispheres. Since the signatures for dawnward moving events are symmetric about the equator, the model predicts more prominent magnetosheath magnetic field FTE signatures on the distant northern dawn and southern dusk flanks than on the dayside magnetopause during intervals of northward and duskward IMF orientation. The dawnward moving events generate out/in bipolar signatures in both magnetosheath hemispheres.

[41] Figure 12b presents the magnetospheric magnetic field component perpendicular to event axes as a function of time and distance from the equatorial plane. Initially, there is a ~10 nT normalized northward magnetospheric magnetic field component perpendicular to the event axis. As the southern half of the event moves across local noon, this component diminishes and then becomes strongly negative, reaching ~−15 nT on the southern dusk flank where magnetospheric magnetic fields point antisunward. The component of the magnetospheric magnetic field perpendicular to the event axis increases to values ~15 nT just north of the magnetic equator where fields point sunward, but diminishes to 0 nT further northward from the equator where fields and event axes are nearly aligned. From these results, we conclude that the magnetic field signatures of magnetospheric FTEs should be larger at off-equatorial flank locations than on the dayside magnetopause during periods of northward and duskward or (by analogy) northward and dawnward IMF orientation. The duskward-moving event connected to the southern ionosphere generates inward/outward bipolar magnetic field signatures near local noon and in the northern dusk magnetosphere but outward/inward bipolar magnetic field signatures in the southern dusk magnetosphere. Note that these signatures are precisely the opposite of those typically observed on the dayside magnetopause: direct outward/inward bipolar signatures north of the equator and reverse inward/outward bipolar signatures south of the equator [e.g., *Cowley*, 1982; *Rijnbeek et al.*, 1984]. Within the framework of the subsolar component

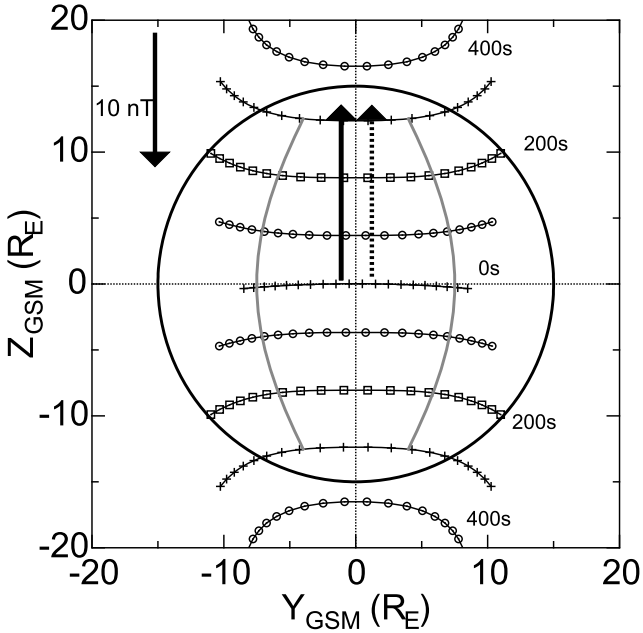

Figure 9. FTE motion away from an equatorial component reconnection curve for a 10 nT southward IMF, solar wind density of 5 cm^{-3}, and solar wind velocity of 400 km s^{-1}. Events connected to the northern and southern hemispheres are shown each 100 s. Crosses, circles, and squares on the events show the locations of points originally separated by 1 R_E. Dashed arrows indicate the northward motion of fluid parcels connected to the Northern Hemisphere. These are the plasma velocities that would be observed by a spacecraft entering the events. Solid arrows indicate the component of these velocities transverse to event axes. These are the velocities that would be determined from timing studies. Gray curves illustrate two magnetosheath magnetic field lines draped against the magnetopause.

reconnection line model, magnetospheric events generated for northward and duskward (or dawnward) IMF orientations are either rare or go unnoticed because their signatures are far weaker than those expected during intervals of southward IMF orientation (Figure 10b). Nevertheless, they have been observed on occasion [*Chandler and Avanov*, 2003].

[42] Figure 12c presents the component of the magnetosheath flow shear perpendicular to the event axis. Initially less than 100 km s^{-1} across the entire length of the event, this component diminishes gradually north of the equator but increases rapidly far below the equator to 300 km s^{-1} in regions where the component of the draped magnetic field perpendicular to the event axis is large. Plasma flow perturbations associated with the event should therefore be most prominent in the southern postnoon magnetosheath. By symmetry, flow perturbations associated with the dawnward moving event should be most prominent in the northern prenoon magnetosheath. As the events move through the magnetosheath at speeds greater than the magnetosheath flow, they generate outward/inward bipolar flow perturbations normal to the nominal magnetopause in the magnetosheath.

[43] Now consider the component of the normalized magnetospheric flow shear perpendicular to the event axis, as shown in Figure 12d. Initially only ~50 km s^{-1}, the shear associated with the duskward moving event increases to as much as ~250 km s^{-1} far south of the equator but remains modest far north of the equator. Corresponding events moving dawnward generate large flow perturbations in the northern dawn magnetosphere but only small perturbations in the southern dawn magnetosphere. The events generate inward/outward flow signatures as they pass magnetospheric observers.

[44] Finally, there are reasons to believe that the plasma depletion layer becomes most prominent when the shear angle between the magnetosheath and magnetospheric magnetic fields falls below 30° [*Phan et al.*, 1994]. As described above, the presence of a depletion layer enhances magnetosheath Alfvén velocities by increasing magnetic field strengths and decreasing magnetosheath densities just outside the magnetopause. Under the assumptions employed in this paper, namely that all FTEs have circular magnetosheath cross sections, the enhanced magnetic field strengths would increase the magnetosheath magnetic field perturbations shown in Figure 12a while the enhanced magnetosheath Alfvén velocities would increase the flow perturbations shown in Figures 12c and 12d. However, were the assumption concerning the fixed shape of the magnetosheath event cross section to be dropped, the enhanced magnetic curvature forces associated with stronger depletion layer magnetic fields would flatten the magnetosheath portion of the event cross section, reducing both magnetic field and plasma perturbations in the magnetosheath.

4. Discussion

[45] This section compares results for each of the orientations described above to extract information concerning the motion and perturbations of FTEs as a function of solar wind conditions.

[46] The subsolar component reconnection curves derived in this paper greatly resemble the reconnection lines predicted by *Sonnerup* [1974] and *Gonzalez and Mozer* [1974] for a planar magnetopause separating uniform magnetosheath and magnetospheric magnetic fields. The reconnection curves presented in this paper are almost straight lines, and, like the reconnection lines for the planar magnetopause, their tilt increases as the magnetosheath magnetic field rotates northward and/or its strength increases to magnetospheric levels. Apparently, the dayside magnetopause is sufficiently planar and the magnetosheath and magnetospheric magnetic fields are sufficiently uniform for the planar models to make quite accurate predictions, not only for IMF orientations transverse to the Sun-Earth line, but also for the Parker spiral IMF orientation.

[47] FTE orientations hardly vary as they move away from the reconnection lines along which they originate. Multipoint spacecraft timing studies [e.g., *Fear et al.*, 2007] can therefore be used to determine not only the orientations of FTEs, but also those of the tilted subsolar component reconnection line as a function of solar wind conditions. The same studies can also provide the component of the event velocity transverse to the event axis, which in general is not

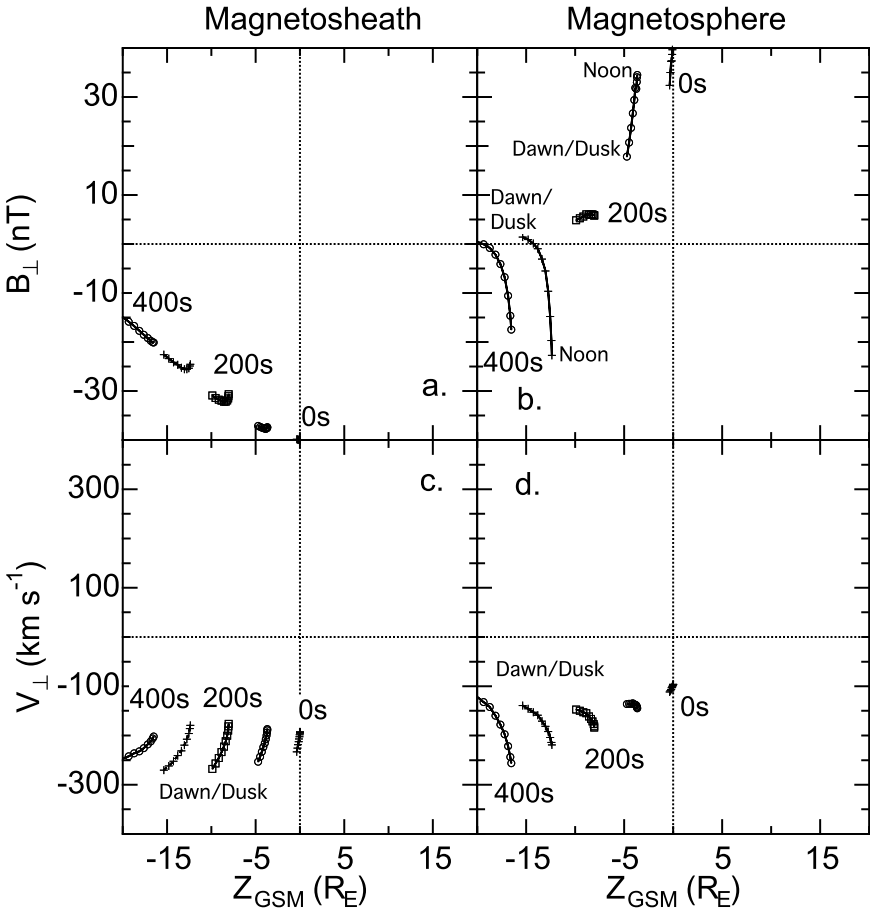

Figure 10. Components of the (a) magnetosheath magnetic field, (b) normalized magnetospheric magnetic field, (c) shear between magnetosheath and event velocities, and (d) normalized shear between magnetospheric and event velocities perpendicular to the event axis as a function of time and distance from the equatorial plane for the 10 nT southward IMF case shown in Figure 9. Magnetospheric values are normalized by balancing magnetosheath and magnetospheric curvature forces to reduce the distances that events with circular magnetosheath cross sections protrude into the magnetosphere. Values are shown for events connected to the Southern Hemisphere at each of the points and each of the times illustrated in Figure 9.

the velocity of the FTE itself, as determined from the *Cooling et al.* [2001] model. The two velocities should only be similar when the Cooling et al. model velocity lies nearly perpendicular to event axes, typically when the IMF points strongly southward (e.g., solid and dashed arrows in Figure 9). For other IMF orientations, the two velocities differ both substantially and systematically (e.g., solid and dashed arrows in Figures 2). During periods of northward and duskward IMF orientation, FTEs connected to the Southern Hemisphere should move northward and duskward, while those connected to the Northern Hemisphere should move southward and dawnward (e.g., Figure 11). However, multispacecraft timing studies of events connected to the Southern Hemisphere should indicate southward and duskward motion, while studies of events connected to the Northern Hemisphere should indicate events moving northward and dawnward. During periods of northward and dawnward IMF orientation, the north/south sense of event motion and the results from timing studies should reverse. Consistent with these predictions for the component reconnection model, *Fear et al.* [2005] used multispacecraft timing methods to infer northward (equatorward) and duskward FTE motion on the southern dusk flank during intervals of strongly northward and dawnward IMF orientation. Under the interpretation proposed in this paper, the events were connected to the Northern Hemisphere and actually moving southward and duskward.

[48] The event motion shown in Figures 2, 4, 6, 9, and 11 is consistent with observed event occurrence patterns as a function of IMF orientation. During periods of duskward IMF orientation, events connected to the northern magnetosphere move dawnward and northward while those connected to the southern magnetosphere move duskward and southward, consistent with the bipolar magnetic field signatures that they generate normal to the magnetopause and their connectivity to the magnetosphere [*Rijnbeek et al.*, 1984; *Daly et al.*, 1984]. Events generated during intervals of strongly southward IMF orientation move poleward over the high-latitude magnetosphere while events generated for northward IMF orientations slip over the flanks. Even if events occurring for southward IMF orientation dominate the dayside population [*Rijnbeek et*

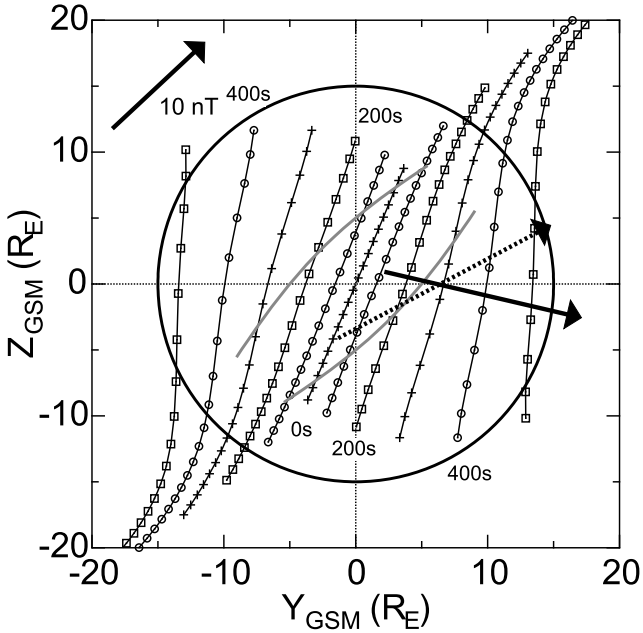

Figure 11. FTE motion away from a tilted subsolar component reconnection curve for a 10 nT northward and duskward IMF with $B_y = B_z = 7.1$ nT, solar wind density of 5 cm^{-3}, and solar wind velocity of 400 km s^{-1}. Events connected to the northern and southern hemispheres are shown each 100 s. Crosses, circles, and squares on the events show the locations of points originally separated by 1 R_E. Dashed arrows indicate the northward and duskward motion of fluid parcels connected to the Southern Hemisphere. These are the plasma velocities that would be observed by a spacecraft entering the events. Solid arrows indicate the component of these velocities transverse to event axes. These are the velocities that would be determined from timing studies. Gray curves illustrate two magnetosheath magnetic field lines draped against the magnetopause.

al., 1984; *Berchem and Russell*, 1984], their preferential removal over the polar caps ensures that populations on the flanks of the magnetosphere will be more evenly balanced between events occurring for northward and southward IMF orientations, as observed [*Kawano and Russell*, 1997a].

[49] Nevertheless, we called attention to the fact that during intervals of northward and duskward IMF orientations the model predicts inward/outward bipolar magnetic field signatures in the northern dusk magnetosphere and outward/inward bipolar magnetic field signatures in the southern dusk magnetosphere. This prediction does not agree with results from statistical surveys incorporating observations from all IMF orientations, suggesting either that the component reconnection line model does not generate events on the dayside magnetopause during intervals of northward and duskward IMF orientation or that the amplitudes of such events are too small to enter into and significantly influence statistical surveys of FTE populations.

[50] Within the framework of the component reconnection model, the corollary is that events on the high-latitude magnetopause must exhibit an exceptionally strong tendency to occur for southward IMF orientations. *Sibeck et al.* [2005] reported that Interball-1 events on the high-latitude magnetopause do tend to occur for southward IMF orientations but did not consider occurrence versus the IMF clock angle. Nevertheless, they showed that magnetosheath magnetic field orientations at the times of the events were almost precisely parallel or antiparallel to the southward magnetospheric magnetic fields poleward of the cusp. Presumably component reconnection on the equatorial magnetopause generated the events that occurred for southward magnetosheath magnetic fields nearly parallel to the southward magnetospheric mantle magnetic fields, whereas local antiparallel reconnection must be invoked to explain those that occurred for northward magnetosheath magnetic field orientations nearly antiparallel to the southward magnetospheric mantle magnetic fields.

[51] The magnetic field perturbations that FTEs generate in the surrounding media depend upon the components of the magnetic field in these media perpendicular to the event axes. Under our assumptions that burst durations do not depend strongly on the shear angle between the magnetosheath and magnetospheric magnetic fields and that magnetosheath cross sections are always circular, we can compare event perturbations predicted for the different cases presented here. The largest perturbation amplitudes (~40 nT) occur in the equatorial magnetosheath and magnetosphere during intervals when the IMF points strongly southward (Figure 10). At these times, event axes run from east to west and lie transverse to both magnetosheath and magnetospheric magnetic field orientations. Perturbation amplitudes diminish as events generated during intervals of southward IMF orientation move poleward into regions of weaker magnetosheath and magnetospheric magnetic fields (Figure 10). Nevertheless, amplitudes in the off-equatorial magnetosheath also remain large (~25 nT at $Z = \pm 15$ R_E). Event amplitudes in the magnetosheath and magnetosphere never exceed ~15 nT at the equator when the IMF points northward and duskward (Figure 12). Since events enter statistical studies on the basis of their perturbations exceeding specified threshold criteria, the results indicate that events occurring for southward IMF orientations will dominate surveys of events on the dayside equatorial magnetopause, as frequently reported [*Berchem and Russell*, 1984; *Rijnbeek et al.*, 1984]. Consistent with these predictions, *Wang et al.* [2005] reported that Cluster observes events with greater amplitudes at high latitudes near local noon than at equatorial latitudes on the flanks of the magnetosphere, and *Wang et al.* [2006] reported a strong tendency for event amplitudes to increase as the southward component of the IMF increases.

[52] Perturbation amplitudes within 5 R_E of the equator diminish as events generated during intervals of duskward IMF orientation move away from the reconnection line (Figures 3, 5, 7, and 8). By contrast, event amplitudes can increase as events generated during intervals of northward and duskward IMF orientation slip around the magnetotail flanks. As illustrated by Figure 12, the perturbations associated with events formed for northward and duskward IMF orientations are initially ~15 nT in the magnetosheath and ~10 nT in the magnetosphere. As time progresses, duskward moving events connected to the Southern Hemisphere create

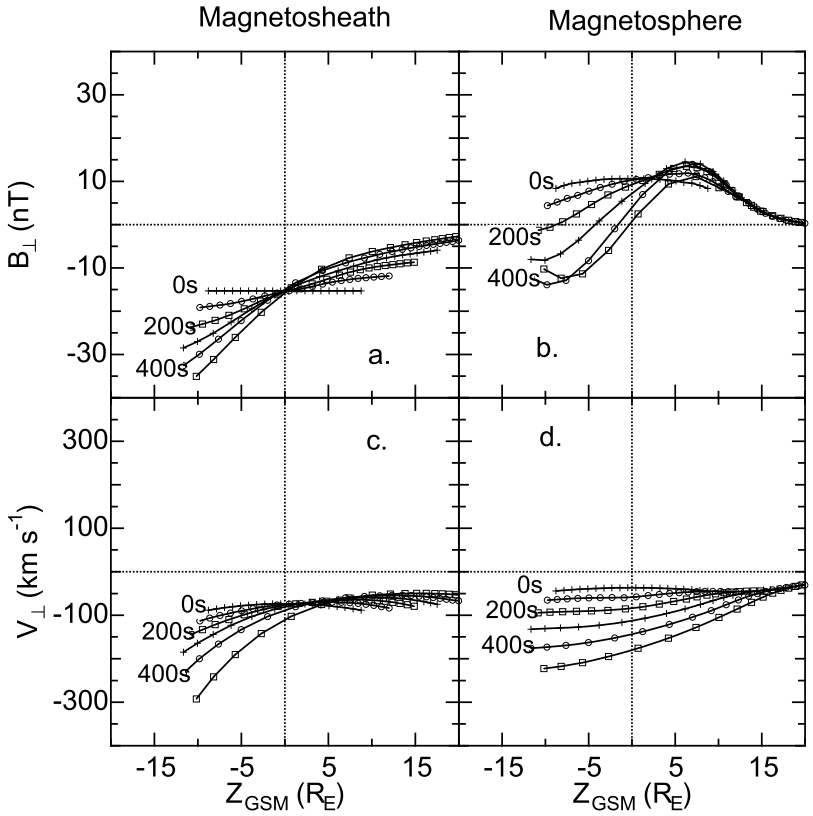

Figure 12. Components of the (a) magnetosheath magnetic field, (b) normalized magnetospheric magnetic field, (c) shear between magnetosheath and event velocities, and (d) normalized shear between magnetospheric and event velocities perpendicular to the event axis as a function of time and distance from the equatorial plane for the 10 nT northward and duskward IMF case shown in Figure 11. Magnetospheric values are normalized by balancing magnetosheath and magnetospheric curvature forces to reduce the distances that events with circular magnetosheath cross sections protrude into the magnetosphere. Values are shown for events connected to the Southern Hemisphere at each of the points and each of the times illustrated in Figure 11.

steadily greater perturbations in the southern postnoon magnetosheath and eventually make ~25 nT perturbations 5 R_E off the equator at T = 400 s in the flank magnetosphere. Because events that occur for northward and duskward IMF orientations become even more prominent as they slip over the dawn and dusk flanks, and events that occur for strongly southward IMF orientations do not reach the flanks, it must be the case that the northward and duskward IMF events play an increasingly important role in the distribution of events on the flanks, consistent with the observations reported by *Kawano and Russell* [1997a].

[53] The most important result regarding the flow perturbations associated with FTEs produced along tilted subsolar reconnection lines is that the events only generate inward/outward flow signatures in the magnetosphere and outward/inward flow signatures in the magnetosheath. Consistent with these predictions, *Korotova et al.* [2009] reported that all magnetospheric events generate inward/outward flow signatures and that a plurality of magnetosheath events generate outward/inward flow signatures. However, many magnetosheath events generate weak or unclear flow signatures, suggesting that they move with speeds near the background magnetosheath flow velocity. A small minority of magnetosheath events generate inward/outward flow signatures, which *Korotova et al.* [2009] interpreted as evidence either for events moving slower than the magnetosheath flow or entries into rotating events.

[54] A detailed inspection of the plots for flow perturbations reveals several other predictions. A comparison of Figures 12 (northward and duskward IMF) and 10 (southward IMF) demonstrates that the flow perturbations for southward IMF events are about twice as large as those for northward and duskward IMF events in the equatorial magnetosheath. In the equatorial magnetosheath, southward IMF events should produce ~200 km s^{-1} shears, while northward and duskward IMF events produce ~100 km s^{-1} shears. In the equatorial magnetosphere, southward IMF events should produce ~100 km s^{-1} shears, while northward and duskward IMF events produce shears that increase from ~50 to 200 km s^{-1} as the events move toward the flanks. If a depletion layer is present predominantly for northward IMF orientations [*Phan et al.*, 1994], then the velocities at which events move during intervals of northward IMF will increase and the flow perturbations for northward/duskward IMF events will become comparable to or larger than those for southward IMF events. The results shown in Figures 3, 5, 7, 8, 10, and 12 indicate a tendency for the perturbation velocities to increase with distance from the equator. If FTEs

form along long reconnection lines, then the most significant velocity perturbations will be observed at high latitudes.

[55] Finally, the model frequently predicts magnetospheric magnetic field perturbations as great as those in the magnetosheath. Although this prediction is consistent with studies indicating approximately equal numbers of magnetosheath and magnetospheric events [*Kawano and Russell*, 1996], it is not consistent with surveys indicating many more magnetosheath than magnetospheric events [*Kuo et al.*, 1995; *Wang et al.*, 2005]. The strong radial gradient in magnetospheric magnetic field strengths may require even greater "normalizing" (or "diminishing") of the magnetospheric plasma flow and magnetic field perturbations, since it means that perturbation amplitudes would decay more rapidly with distance into the magnetosphere than into the magnetosheath.

5. Summary and Conclusions

[56] We assumed that FTEs are generated by near-instantaneous component reconnection along one or more tilted reconnection curves $\leq 19\ R_E$ long that pass through the immediate vicinity of the subsolar magnetopause and parallel to the magnetopause current vector. The tilts of these curves for a paraboloid magnetopause separating realistic magnetosheath and magnetospheric magnetic fields are similar to those predicted for an idealized planar magnetopause separating uniform magnetic fields.

[57] The locations where FTE magnetic field lines cross the magnetopause move in response to pressure gradient and magnetic curvature forces. We employed the *Cooling et al.* [2001] model to determine the motion of these field lines and used this information to determine consecutive event orientations and locations. We then used the components of the magnetic field and flow velocity perpendicular to the event axes to estimate the perturbations generated by the events in the ambient media.

[58] We showed that FTEs generated during periods of southward IMF orientation move rapidly over the polar caps, those generated during periods of northward IMF orientation slip slowly around the magnetospheric flanks, and those generated during periods of duskward IMF orientation move either northward and dawnward or southward and duskward. When the IMF lies in a Parker spiral, the magnetosheath magnetic field splays against the prenoon magnetopause but drapes against the postnoon magnetopause, and events move antisunward more slowly prior to local noon than after local noon. Events depart from the dayside magnetopause more rapidly when magnetosheath magnetic field strengths are greater, as might be the case when IMF strengths are greater or a depletion layer is present (typically during intervals of northward IMF). Event velocities typically differ from the velocities determined from multispacecraft timing analyses. Broad stretches of the antisunward moving FTEs retain their initial orientation, namely that of the subsolar reconnection line. Because event lengths grow with time, faster-moving events occurring for southward IMF orientations do not grow to lengths as great as slower-moving events occurring for northward IMF orientations before they depart the dayside magnetopause.

[59] On the dayside equatorial magnetopause, events generate far greater magnetic field perturbations for southward IMF orientations than for northward IMF orientations. Consequently even if events are equally common for northward and southward IMF orientations, events occurring for southward IMF orientations will dominate statistical surveys of dayside events in which events are selected on the basis of amplitude thresholds. However, the motion of events generated for southward IMF orientation over the polar caps, the motion of events generated for northward IMF orientations toward the flanks, and the fact that events moving toward the flanks enter a region of differing (Sun-aligned) magnetospheric magnetic field orientations where they generate greater magnetic field perturbations should all conspire to make events generated for northward IMF orientations as common, and as prominent, as those for southward IMF orientations on the flanks of the magnetosphere.

[60] The flow perturbations generated by FTEs in both the magnetosheath and magnetosphere increase with increasing IMF strength. Flow perturbations are greatest in the equatorial dayside magnetosheath for southward IMF orientations because the magnetosheath magnetic field lies nearly perpendicular to event axes. In general, both magnetosheath and magnetospheric flow perturbations are greater at off-equatorial locations than at the equator.

[61] **Acknowledgments.** Work at GSFC was funded by the NASA Heliophysics Guest Investigator program and the THEMIS and MMS projects. We thank Y. Wang, S. Eriksson, and both referees for helpful comments. D.G.S. thanks the staff of the International Space Science Institute in Bern, Switzerland, for their hospitality during two visits by a group working on FTEs.

[62] Zuyin Pu thanks Robert Fear and another reviewer for their assistance in evaluating this manuscript.

References

Alexeev, I. I., E. S. Belenkaya, S. U. Bobrovnikov, and V. V. Kalegaev (2003), Modeling of the electromagnetic field in the interplanetary space and in the Earth's magnetosphere, *Space Sci. Rev.*, *107*, 7–26, doi:10.1023/A:1025542915800.

Berchem, J., and C. T. Russell (1984), Flux transfer events on the magnetopause: Spatial distribution and controlling factors, *J. Geophys. Res.*, *89*, 6689–6703, doi:10.1029/JA089iA08p06689.

Berchem, J., J. Raeder, and M. Ashour-Abdalla (1995), Magnetic flux ropes at the high-latitude magnetopause, *Geophys. Res. Lett.*, *22*, 1189–1192, doi:10.1029/95GL01014.

Chandler, M. O., and L. A. Avanov (2003), Observations at low latitudes of magnetic merging signatures within a flux transfer event during a northward interplanetary magnetic field, *J. Geophys. Res.*, *108*(A10), 1358, doi:10.1029/2003JA009852.

Cooling, B. M. A., C. J. Owen, and S. J. Schwartz (2001), Role of the magnetosheath flow in determining the motion of open flux tubes, *J. Geophys. Res.*, *106*, 18,763–18,775, doi:10.1029/2000JA000455.

Cowley, S. W. H. (1976), Comments on the merging of nonantiparallel magnetic fields, *J. Geophys. Res.*, *81*, 3455–3458, doi:10.1029/JA081i019p03455.

Cowley, S. W. H. (1982), The causes of convection in the Earth's magnetosphere: A review of developments during the IMS, *Rev. Geophys. Space Phys.*, *20*, 531–565, doi:10.1029/RG020i003p00531.

Cowley, S. W. H., and M. Lockwood (1992), Excitation and decay of solar wind-driven flows in the magnetosphere-ionosphere system, *Ann. Geophys.*, *10*, 103–115.

Cowley, S. W. H., and C. J. Owen (1989), A simple illustrative model of open flux tube motion over the dayside magnetopause, *Planet. Space Sci.*, *37*, 1461–1475, doi:10.1016/0032-0633(89)90116-5.

Crooker, N. U. (1979), Dayside merging and cusp geometry, *J. Geophys. Res.*, *84*, 951–959, doi:10.1029/JA084iA03p00951.

Crooker, N. U. (1985), A split separator line merging model of the dayside magnetopause, *J. Geophys. Res.*, *90*, 12,104–12,110, doi:10.1029/JA090iA12p12104.

Crooker, N. U., T. E. Eastman, and G. S. Stiles (1979), Observation of plasma depletion in the magnetosheath at the dayside magnetopause, *J. Geophys. Res.*, *84*, 869–874, doi:10.1029/JA084iA03p00869.

Crooker, N. U., G. L. Siscoe, and F. R. Toffoletto (1990), A tangent subsolar merging line, *J. Geophys. Res.*, *95*, 3787–3793, doi:10.1029/JA095iA04p03787.

Daly, P. W., M. A. Saunders, R. P. Rijnbeek, N. Sckopke, and C. T. Russell (1984), The distribution of reconnection geometry in flux transfer events using energetic ion, plasma and magnetic data, *J. Geophys. Res.*, *89*, 3843–3854, doi:10.1029/JA089iA06p03843.

Ding, D.-Q., L.-C. Lee, and Z.-W. Ma (1991), Different FTE signatures initiated by the bursty single X line reconnection and the multiple X line reconnection at the dayside magnetopause, *J. Geophys. Res.*, *96*, 57–66, doi:10.1029/90JA01989.

Dorelli, J. C., A. Bhattacharjee, and J. Raeder (2007), Separator reconnection at Earth's dayside magnetopause under generic northward interplanetary magnetic field conditions, *J. Geophys. Res.*, *112*, A02202, doi:10.1029/2006JA011877.

Dunlop, M. W., et al. (2005), Coordinated Cluster/Double Star observations of dayside reconnection signatures, *Ann. Geophys.*, *23*, 2867–2875.

Farrugia, C. J., R. C. Elphic, D. J. Southwood, and S. W. H. Cowley (1988), Field and flow perturbations outside the reconnected field line region in flux transfer events: Theory, *Planet. Space Sci.*, *35*, 227–240, doi:10.1016/0032-0633(87)90091-2.

Fear, R. C., A. N. Fazakerley, C. J. Owen, and E. A. Lucek (2005), A survey of flux transfer events observed by Cluster during strongly northward IMF, *Geophys. Res. Lett.*, *32*, L18105, doi:10.1029/2005GL023811.

Fear, R. C., S. E. Milan, A. N. Fazakerley, C. J. Owen, T. Asikainen, M. G. G. T. Taylor, E. A. Lucek, H. Reme, I. Dandouras, and P. W. Daly (2007), Motion of flux transfer events: A test of the Cooling model, *Ann. Geophys.*, *25*, 1669–1690.

Fear, R. C., S. E. Milan, A. N. Fazakerley, E. A. Lucek, S. W. H. Cowley, and I. Dandouras (2008), The azimuthal extent of three flux transfer events, *Ann. Geophys.*, *26*, 2353–2369.

Fear, R. C., S. E. Milan, E. A. Lucek, S. W. H. Cowley, and A. N. Fazakerley (2009), Mixed azimuthal scales of flux transfer events, in *The Cluster Active Archive: Studying the Earth's Space Plasma Environment*, edited by H. Laakso, M. Taylor, and P. Escoubet, pp. 389–398, Springer, Dordrecht, Netherlands.

Fedder, J. A., S. P. Slinker, J. G. Lyon, and C. T. Russell (2002), Flux transfer events in global numerical simulations of the magnetosphere, *J. Geophys. Res.*, *107*(A5), 1048, doi:10.1029/2001JA000025.

Fuselier, S., S. M. Petrinec, and K. Trattner (2000), Cusp observations of high- and low-latitude reconnection for northward interplanetary magnetic field, *J. Geophys. Res.*, *105*, 253–266, doi:10.1029/1999JA900422.

Gonzalez, W. D., and F. S. Mozer (1974), A quantitative model for the potential resulting from reconnection with an arbitrary interplanetary magnetic field, *J. Geophys. Res.*, *79*, 4186–4194, doi:10.1029/JA079i028p04186.

Kawano, H., and C. T. Russell (1996), Survey of flux transfer events observed with the ISEE 1 spacecraft: Rotational polarity and the source region, *J. Geophys. Res.*, *101*, 27,299–27,308, doi:10.1029/96JA02703.

Kawano, H., and C. T. Russell (1997a), Survey of flux transfer events observed with the ISEE 1 spacecraft: Dependence on the interplanetary magnetic field, *J. Geophys. Res.*, *102*, 10,307–11,313.

Kawano, H., and C. T. Russell (1997b), Cause of postterminator flux transfer events, *J. Geophys. Res.*, *102*, 27,029–27,038, doi:10.1029/97JA02139.

Kobel, E., and E. O. Flückiger (1994), A model of the steady state magnetic field in the magnetosheath, *J. Geophys. Res.*, *99*, 23,617–23,622, doi:10.1029/94JA01778.

Korotova, G. I., D. G. Sibeck, and T. Rosenberg (2009), Geotail observations of FTE velocities, *Ann. Geophys.*, *27*, 83–92.

Kuo, H., C. T. Russell, and G. Le (1995), Statistical studies of flux transfer events, *J. Geophys. Res.*, *100*, 3513–3519, doi:10.1029/94JA02498.

Kuznetsova, M. M., D. G. Sibeck, M. Hesse, L. Rastätter, G. Toth, and A. Ridley (2009), Cavities of weak magnetic field strength in the wake of FTEs: Results from global magnetospheric MHD simulations, *Geophys. Res. Lett.*, *36*, L10104, doi:10.1029/2009GL037489.

Lee, L.-C., and Z.-F. Fu (1985), A theory of magnetic flux transfer at the Earth's magnetopause, *Geophys. Res. Lett.*, *12*, 105–108, doi:10.1029/GL012i002p00105.

Lockwood, M., and M. N. Wild (1993), On the quasi-periodic nature of magnetopause flux transfer events, *J. Geophys. Res.*, *98*, 5935–5940, doi:10.1029/92JA02375.

Lockwood, M., S. W. H. Cowley, P. E. Sandholt, and R. P. Lepping (1990), The ionospheric signatures of flux transfer events and solar wind dynamic pressure changes, *J. Geophys. Res.*, *95*, 17,113–17,135, doi:10.1029/JA095iA10p17113.

Luhmann, J. G., R. J. Walker, C. T. Russell, N. U. Crooker, J. R. Spreiter, and S. S. Stahara (1984), Patterns of potential merging sites on the dayside magnetopause, *J. Geophys. Res.*, *89*, 1739–1742, doi:10.1029/JA089iA03p01739.

Milan, S. E., M. Lester, S. W. H. Cowley, and M. Brittnacher (2000), Convection and auroral response to a southward turning of the IMF: Polar UVI, CUTLASS, and IMAGE signatures of transient magnetic flux transfer at the magnetopause, *J. Geophys. Res.*, *105*, 15,741–15,756, doi:10.1029/2000JA900022.

Omidi, N., and D. G. Sibeck (2007), Flux transfer events in the cusp, *Geophys. Res. Lett.*, *34*, L04106, doi:10.1029/2006GL028698.

Phan, T.-D., G. Paschmann, W. Baumjohann, N. Sckopke, and H. Lühr (1994), The magnetosheath region adjacent to the dayside magnetopause: AMPTE/IRM observations, *J. Geophys. Res.*, *99*, 121–141, doi:10.1029/93JA02444.

Phan, T.-D., et al. (2000), Extended magnetic reconnection at the Earth's magnetopause from detection of bi-directional jets, *Nature*, *404*, 848–850, doi:10.1038/35009050.

Phan, T.-D., H. Hasegawa, M. Fujimoto, M. Øireoset, T. Mukai, and R. P. Lin (2006), Simultaneous Geotail and Wind observations of reconnection at the subsolar and flank magnetopause, *Geophys. Res. Lett.*, *33*, L09104, doi:10.1029/2006GL025756.

Raeder, J. (2006), Flux transfer events: 1. Generation mechanism for strong southward IMF, *Ann. Geophys.*, *24*, 381–392.

Rijnbeek, R. P., S. W. H. Cowley, D. J. Southwood, and C. T. Russell (1984), A survey of dayside flux transfer events observed by ISEE 1 and 2 magnetometer, *J. Geophys. Res.*, *89*, 786–800, doi:10.1029/JA089iA02p00786.

Russell, C. T., and R. C. Elphic (1978), Initial ISEE magnetometer results: Magnetopause observations, *Space Sci. Rev.*, *22*, 681–715, doi:10.1007/BF00212619.

Russell, C. T., Y. L. Wang, and J. Raeder (2003), Possible dipole tilt dependence of dayside magnetopause reconnection, *Geophys. Res. Lett.*, *30*(18), 1937, doi:10.1029/2003GL017725.

Saunders, M. A., M. P. Freeman, D. J. Southwood, S. W. H. Cowley, M. Lockwood, J. C. Samson, C. J. Farrugia, and T. J. Hughes (1992), Dayside ionospheric convection changes in response to long-period magnetic field oscillations: Determination of the ionospheric phase velocity, *J. Geophys. Res.*, *97*, 19,373–19,380, doi:10.1029/92JA01383.

Scholer, M. (1988), Magnetic flux transfer at the magnetopause based on single X line bursty reconnection, *Geophys. Res. Lett.*, *15*, 291–294, doi:10.1029/GL015i004p00291.

Shue, J.-H., J.-K. Chao, H.-C. Fu, C. T. Russell, P. Song, K. K. Khurana, and H. J. Singer (1997), A new functional form to study the solar wind control of the magnetopause size and shape, *J. Geophys. Res.*, *102*, 9497–9512, doi:10.1029/97JA00196.

Sibeck, D. G. (2009), Concerning the occurrence pattern of flux transfer events on the dayside magnetopause, *Ann. Geophys.*, *27*, 895–903.

Sibeck, D. G., G. I. Korotova, V. Petrov, V. Styazhkin, and T. J. Rosenberg (2005), Flux transfer events on the high-latitude magnetopause: Interball-1 observations, *Ann. Geophys.*, *23*, 1–11.

Sibeck, D. G., M. Kuznetsova, V. Angelopoulos, K.-H. Glassmeier, and J. P. McFadden (2008), Crater FTEs: Simulation results and THEMIS observations, *Geophys. Res. Lett.*, *35*, L17S06, doi:10.1029/2008GL033568.

Sonnerup, B. U. Ö. (1974), Magnetopause reconnection rate, *J. Geophys. Res.*, *79*, 1546–1549, doi:10.1029/JA079i010p01546.

Southwood, D. J., C. J. Farrugia, and M. A. Saunders (1988), What are flux transfer events? *Planet. Space Sci.*, *36*, 503–508, doi:10.1016/0032-0633(88)90109-2.

Spreiter, J. R., A. L. Summers, and A. Y. Alksne (1966), Hydromagnetic flow around the magnetosphere, *Planet. Space Sci.*, *14*, 223–250, doi:10.1016/0032-0633(66)90124-3.

Swisdak, M., and J. F. Drake, J. F. (2007), Orientation of the reconnection X-line, *Geophys. Res. Lett.*, *34*, L11106, doi:10.1029/2007GL029815.

Trattner, K. J., S. A. Fuselier, and S. M. Petrinec (2004), Location of the reconnection line for northward interplanetary magnetic field, *J. Geophys. Res.*, *109*, A03219, doi:10.1029/2003JA009975.

Trattner, K. J., J. S. Mulcock, S. M. Petrinec, and S. A. Fuselier (2007), Probing the boundary between antiparallel and component reconnection during southward interplanetary magnetic field condition, *J. Geophys. Res.*, *112*, A08210, doi:10.1029/2007JA012270.

Wang, Y. L., et al. (2005), Initial results of high-latitude magnetopause and low-latitude flank flux transfer events from 3 years of Cluster observations, *J. Geophys. Res.*, *110*, A11221, doi:10.1029/2005JA011150.

Wang, Y. L., R. C. Elphic, B. Lavraud, M. G. G. T. Taylor, J. Birn, C. T. Russell, J. Raeder, H. Kawano, and X. X. Zhang (2006), Dependence

of flux transfer events on solar wind conditions from 3 years of Cluster observations, *J. Geophys. Res.*, *111*, A04224, doi:10.1029/2005JA011342.
Wild, J. A., et al. (2003), Coordinated interhemispheric SuperDARN radar observations of the ionospheric response to flux transfer events observed by the Cluster spacecraft at the high latitude magnetopause, *Ann. Geophys.*, *21*, 1807–1826.
Wild, J. A., et al. (2005), Simultaneous in-situ observations of the signatures of dayside reconnection at the high- and low-latitude magnetopause, *Ann. Geophys.*, *23*, 445–460.
Wild, J. A., S. E. Milan, J. A. Davies, M. W. Dunlop, D. M. Wright, C. M. Carr, A. Balogh, H. Reme, A. N. Fazakerley, and A. Marchaudon (2007), On the location of magnetic reconnection during an interval of duskward oriented IMF, *Ann. Geophys.*, *25*, 219–238.

R.-Q. Lin, Carderock Division, Naval Surface Warfare Center, 9500 MacArthur Blvd., West Bethesda, MD 20817, USA.
D. G. Sibeck (corresponding author), NASA Goddard Space Flight Center, Code 674, 8800 Greenbelt Rd., Greenbelt, MD 20771, USA. (david.g.sibeck@nasa.gov)